4.2

Determinants of iron accumulation in deep grey matter of multiple sclerosis patients

Multiple Sclerosis (2014) 20: 1692-1698

Stefan Ropele
Iris D Kilsdonk
Mike P Wattjes
Christian Langkammer
Wolter L de Graaf
Jette L Frederiksen
Henrik BW Larsson
Marios Yiannakas
Claudia AM Wheeler-Kingshott
Christian Enzinger
Michael Khalil
Mara A Rocca
Till Sprenger
Michael Amann
Ludwig Kappos
Massimo Filippi
Alex Rovira
Olga Ciccarelli
Frederik Barkhof
Franz Fazekas

Abstract

Background

Iron accumulation in deep grey matter (GM) structures is a consistent finding in multiple sclerosis (MS) patients. This study focused on the identification of independent determinants of iron accumulation using R2* mapping.

Subjects and methods

Ninety-seven MS patients and 81 healthy controls were included in this multicenter study. R2* mapping was performed on 3T MRI systems. R2*in deep GM was corrected for age and was related to disease duration, disability, T2 lesion load and brain volume.

Results

Compared to controls, R2* was increased in all deep GM regions of MS patients except the globus pallidus and the substantia nigra. R2* increase was most pronounced in the progressive stage of the disease and independently predicted by disease duration and disability. Reduced cortical volume was not associated with iron accumulation in the deep GM with the exception of the substantia nigra and the red nucleus. In lesions, R2* was inversely correlated with disease duration and higher total lesion load.

Conclusion

Iron accumulation in deep GM of MS patients is most strongly and independently associated with duration and severity of the disease. Additional associations between cortical GM atrophy and deep GM iron accumulation appear to exist in a region specific manner.

Introduction

There is convincing evidence that iron levels are elevated in specific brain regions of MS patients. While several MRI studies have contributed to this evidence mainly for deep gray matter (GM),[1-8] the extent and significance of iron accumulation in and around MS lesions is still a matter of debate. Triggered by histopathologic studies,[9,10] recent susceptibility based MRI studies have also suggested an increase of iron in chronic lesions,[11,12] or in newly developing MS lesions that persists for several months.[13] In contrast, iron in normal appearing white matter (WM) has been suggested to decrease due to changes in oligodendrocytes and myelin with increasing disease duration.[14]

The mechanism(s) behind the changes in iron concentration are not well understood. Previous MRI studies have suggested that disability[1-4] and disease duration[5,7] are potential determinants of iron accumulation in the basal ganglia while WM damage visible on conventional MRI did not appear to play a role. More recent data also suggests a relation between basal ganglia iron concentrations and regional[15] and cortical atrophy.[6,7] Unfortunately many of these studies used MR techniques with different sensitivity for iron which makes it difficult to compare their results. An additional limitation comes from the fact that most studies have focused on patients presenting the clinically isolated syndrome (CIS) suggestive of MS and early remitting relapsing (RR) MS and thus have mainly focused on rather early disease courses. Even more importantly, results have been reported exclusively from single centers so far. However, the practicability of iron measurements at multiple sites would be an important issue if such metrics should become clinically meaningful.

We therefore placed this study within the MAGNIMS network (http://www.magnims.eu) and decided for mapping the transverse relaxation rate R2* among the many available options to assess iron levels with MRI, mainly because the gradient echo sequence underlying this technique is readily available on clinical MRI systems and allows whole brain mapping within a clinically feasible acquisition time.[16] R2* mapping has also been validated in a correlation study against chemical determination of iron levels17 and iron-staining.[18] Furthermore, we aimed to recruit a cohort with a broad clinical spectrum of MS including also later and advanced stages. Additionally, we applied a new correction scheme to account for the non-linear effects of age on iron accumulation,[19] thereby attempting to increase the specificity of our findings.

Methods

MS Patients and Healthy Controls

This study was conducted within the MAGNIMS (Magnetic Resonance Imaging in MS) network. The study was approved by the institutional review boards at each of the participating centers and written informed consent was obtained from all participants. Seven centers included 97 MS patients (65 female / 32 male, aged 17 – 63 years, mean age 37.4 years) and 81 healthy control subjects (50 female / 31male, aged 18 – 57 years, mean age 31.6 years). Every center recruited between 10 patients and 23 patients. For inclusion into the study, controls had to be free of any neurological disease or cognitive deficits. Regarding the MS patients, there were no inclusion or exclusion criteria dealing with the Expanded Disability Status Scale (EDSS) score, disease duration and treatment. Table 1 provides an overview on the demographic and clinical characteristics of the included MS patients and healthy controls.

Table 1. Characteristics of MS patients and controls

	n	sex (F/M)	age range (mean)	disease duration range (mean)	EDSS	T2 lesion load (cm^3)	cortical GM volume(cm^3)	total WM volume (cm^3)
MS	97	65/32	17-63 (37.4)	1-28 (8.4)	0-7.5 (3.1)	7.3 (9.4)	604.3 (44.9)	700.7 (48.9)
RRMS	83	58/25	17-55 (35.9)	1-27 (7.8)	0-7 (2.8)	7.1 (9.4)	607.9 (46.0)	705.7 (47.7)
SPMS	7	2/5	35-59(43.7)	3-28 (12)	1.5-7.5(4.5)	7.5 (8.5)	577.8 (20.2)	675.7 (41.4)
PPMS	7	5/2	34-63 (49.4)	8-19 (13.1)	2.5-7 (4.2)	10.2 (10.9)	584.7 (42.4)	662.7 (51.3)
Controls	81	50/31	18-57 (31.6)	n.a.	n.a.	n.a.	631.0 (54.6)	731.8 (42.3)

Values in parentheses represent the standard deviation

Magnetic Resonance Imaging

All study participants underwent conventional MRI and R2* mapping on 3 Tesla whole-body MR systems (Tim Trio, Siemens Medical System; HDXT, General Electrics; Achieva, Philips Medical Systems).The standardized MRI protocol included a T2 weighted fast spin echo sequence and an axial fluid attenuated inversion recovery (FLAIR) T2 weighted fast spin echo sequence (1x1 mm^2 in-plane resolution, 3 mm slice thickness, no slice gap). For assessing brain volume, a high resolution spoiled 3D T1-weighted gradient echo sequence with magnetization preparation (MPRAGE, TFE, or IR prepped SPGR) with 1mm isotropic resolution and whole brain coverage was performed. For R2* mapping, a spoiled 3D gradient echo sequence (FLASH, T1FFE, or SPGR) with two echoes was used (repetition time = 30 ms, flip angle = 15°, TE1 = 4.92 ms, TE2 = 24.6 ms, bandwidth 160 – 200 Hz/pixel, in-plane resolution =1x1mm^2, slice thickness = 2mm). The echo times of the gradient echo sequence were chosen to maximize the sensitivity for physiological variations in iron concentration in the structures investigated.

R2* mapping

Based on the signal of both gradient echoes, maps of the R2* relaxation rate were calculated pixel-wise using the equation

$$R2^* = (TE_2 - TE_1)\ln(S_{TE1}/S_{TE2}) \qquad [1]$$

where TE_1 and TE_2 denote the echo time of the first and second echo, and S_{TE1} and S_{TE2} denote the signal intensity of the corresponding echoes, respectively (figure 1). Equation [1] implies that the loss of the transverse magnetization in a gradient echo sequence follows a single exponential decay.

Image Analysis

R2* was assessed in MS lesions and in different deep GM regions. Outlining of the MS lesions was done on FLAIR images by a single rater (IK) using a semiautomatic region growing algorithm with local thresholding. The deep GM regions were also assessed on FLAIR images by manual outlining and included the caudate nucleus, the putamen, the globus pallidus, the dentate nucleus, the red nucleus, and the substantia nigra. The putamen was separated into an anterior and posterior part to account for the reported functional differences between these regions.[20,21]The border between these two regions was defined as the line passing through the anterior commissure. FLAIR and gradient echo images were registered to the high resolution T1 images using affine registration as implemented within FLIRT (part of FSL version 5.0, http://

fsl.fmrib.ox.ac.uk/fsl). The resulting transformation matrix was then used to superimpose the FLAIR masks onto the R2* maps. To reduce partial volume effects, the masks were eroded by one voxel before the mean R2* value was calculated for each region. Brain tissue volume was measured on the 3D-T1 images using SIENAX which is also part of FSL. We generated separate volumes of total GM, cortical GM, total white matter and of the ventricular CSF and normalized them for subject head size. The 3D-T1 images were also used for automatically segmenting deep GM structures such as the caudate nucleus, the globus pallidus and the dendate nucleus with FIRST, which is a segmentation and registration algorithm based on deformable models from FSL. Other structures investigated in this work could not be segmented with FIRST and were therefore not considered for volumetric analysis. The total T2 lesion load was calculated for each patient by multiplying the area of all T2 lesion masks by the slice thickness of the FLAIR scans. R2* mapping and all image analysis steps were done at the Department of Neurology of the Medical University of Graz.

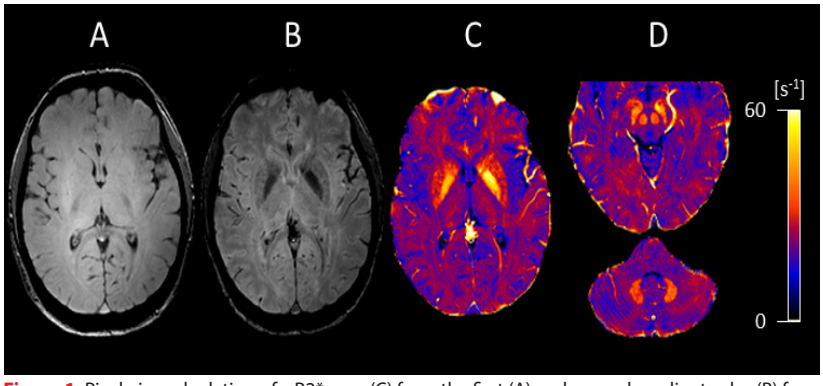

Figure 1. Pixelwise calculation of a R2* map (C) from the first (A) and second gradient echo (B) from a multiple sclerosis (MS) patient using equation [1]. The substantia nigra, the red nucleus, and the dendate nucleus can clearly be identified on corresponding maps (D).

Statistical Analysis

Statistical analyses were performed using STATISTICA 7 (StatSoft, Tusla, OK). A Mann-Whitney U test was performed to test for pairwise differences in R2* between MS phenotypes and controls. A Student's t-test was performed to assess gender related differences in regional R2*. Depending on the statistical distribution of the data, Spearman and Pearson correlations served to calculate the correlation coefficients between R2* in deep GM, clinical data and brain volume. Following correlation analyses, a stepwise linear regression model was used to identify independent determinants of iron accumulation in deep GM of the entire MS cohort. Variables showing a significant correlation with deep GM R2* rates in the Pearson or Spearman correlation analyses were then added as independent variables. Variables included in the regression analysis were disease duration, EDSS, cortical GM volume, and white matter volume. After starting with the variable that showed the highest R2, the remaining variables were stepwise added but remained in the model only if R2 of the model could be significantly increased.

Age is the strongest independent determinant of iron accumulation in deep GM but the relationship is non-linear19 which can affect the multiple regression analysis. Therefore, all analyses were performed with age corrected R2* values that were obtained applying a previously

proposed approach.[22] In short, an exponential saturation function with age as independent variable was fitted into the R2* data for each structure. Data to find the age dependency were taken from the control subjects only. After obtaining the parameter of the resulting curve, all R2* data were adjusted to 32 years which was the mean age of the healthy controls. Consequently, age was not included in the regression analysis as covariate. A p-value of less than 0.05 was considered as statistically significant.

Results

Compared to healthy controls, MS patients showed significantly increased R2* values in all deep GM regions, with the exception of the globus pallidus and the substantia nigra (table 2). Overall, PP and SP MS patients had significantly higher R2* values in all regions compared to RR patients, while no difference was found between the PP and SP MS groups. Figure 2 illustrates the distribution of R2* values in the putamen across MS patients and controls. In the correlation analyses, disease duration, EDSS, and brain volume showed a significant effect on age corrected R2* values in deep GM, while T2 lesion load and gender had no effect.

Table 2. Regional R2* rates and their association with brain volume, disability, and disease duration

	Regional R2*				Correlation		Multiple regression model		
	HC [s^{-1}]	RR [s^{-1}]	SP [s^{-1}]	PP [s^{-1}]	cortical GM volume r	WM volume r	EDSS beta	disease duration beta	overall effect size R
R2* caudate nucleus	21.1 (2.4)	22.7 (3.6)	21.9 (2.9)	27.8 (6.7)	n.s.	n.s.	n.s.	n.s.	n.s.
R2* putamen	25.8 (1.9)	26.4 (2.3)	28.3 (1.8)	29.3 (3.2)	n.s.	n.s.	0.21	0.22	0.32 (p=0.01)
anterior	24.9 (2.2)	25.6 (3.0)	27.0 (1.9)	27.7 (3.1)	n.s.	n.s.	0.25	0.32	0.46 (p<0.01)
posterior	26.9 (2.8)	27.7 (3.3)	29.8 (2.3)	33.2 (4.8)	n.s.	n.s.	n.s.	0.20	0.25 (p=0.04)
R2* globus pallidus	37.6 (4.6)	37.3 (4.7)	43.4 (4.7)	39.4 (5.3)	n.s.	-0.22	0.27	0.28	0.35 (p<0.01)
R2* substantia nigra	37.1 (4.6)	36.8 (5.7)	46.4 (6.8)	38.5 (5.1)	-0.43	-0.37	0.33	n.s.	0.34 (p=0.03)
R2* red nucleus	32.6 (3.8)	33.1 (4.5)	38.0 (3.5)	38.3 (3.9)	-0.33	-0.33	0.35	n.s.	0.37 (p<0.01)
R2* dentate nucleus	29.5 (3.9)	31.0 (4.8)	36.2 (3.3)	36.6 (6.2)	n.s.	-0.22	0.36	0.27	0.50 (p<0.001)

The correlation and regression analysis was performed for the entire MS cohort

The effects of brain volumes on R2* values were more heterogeneous than those of EDSS or disease duration. Cortical GM volume was negatively associated with R2* in the substantia nigra (r=-0.43) and red nucleus (r=-0.25) (table 2 and figure 3). In parallel, white matter volume negatively scaled with R2* in the substantia nigra (r=-0.37) and red nucleus (r=-0.33), but also in the globus pallidus (r=-0.22) and dentate nucleus (r=-0.22). A similar relationship was found for white matter volume in healthy controls with a correlation coefficient of -0.30 for the globus pallidus and -0.28 for the substantia nigra. In contrast to MS patients, healthy controls showed a positive association between cortex volume and R2* in the putamen (r=0.22) and red nucleus (r=0.26). No associations were found between the volumes of the caudate nucleus, the globus pallidus and the dendate nucleus, and R2*.

The multiple regression models revealed EDSS and disease duration as the only independent determinants of iron accumulation in deep GM. Results for each region are listed in table 2. The caudate nucleus was the only structure where R2* did not show any association with disability and disease duration in the MS group.

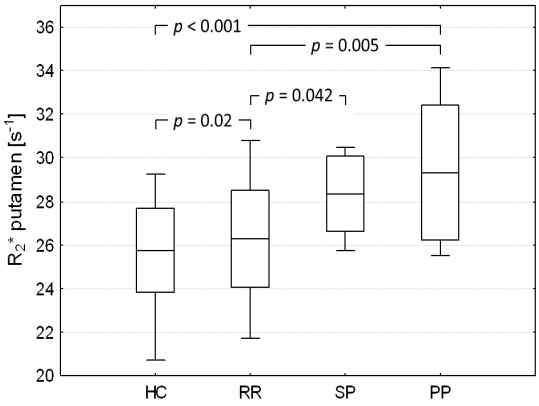

Figure 2. Distribution of R2* in the putamen across healthy controls and different phenotypes of multiple sclerosis (MS). MS patients had higher iron levels than healthy controls with highest concentrations in PP: primary progressive; SP: secondary progressive MS.

Calculation of lesional R2* was based on the T2-hypointense lesion maps outlined on the FLAIR images and did not entail age-correction. An age correction of R2* was not possible because effects other than age-dependent iron accumulation can affect regional R2* in WM even in normal controls. In line with these considerations, we found no significant relationship between lesional R2* and age. However, multiple regression analysis revealed that longer disease duration (r=-0.34, p=0.003) and higher T2 lesion load (r=-0.38, p=0.0002) were associated with decreased R2* in MS lesions.

Discussion

This multi-center study confirms that MS patients show increased iron levels in nearly all deep GM areas when compared to healthy controls. Furthermore, our results indicate that advancing disease reflected by disease duration and disability are the main determinants of iron accumulation, a finding that was not consistent in previous studies. Our findings are also not distorted by age effects as we used a previously developed correction scheme to account for this factor.[22] This scheme considers the non-linear age related accumulation of iron in the brain which in most deep gray matter structures of normal individuals starts to reach a plateau in the fourth decade of life.[19] As the thalamus does not follow this pattern it was not considered in our analysis. Our measurements were based on R2*, as R2* mapping is simple, robust, and does not need any internal reference such as quantitative susceptibility mapping and therefore is more suitable in a multicenter study.[23,24]

In the brain, iron is needed for many processes including oxygen transport, cellular maintenance and metabolism, and for providing energy.[25,26] However, it is unclear why there is a steady accumulation of iron in deep GM even in normal ageing subjects and also how iron is distributed between neurons and glia. Loading of the intracellular ferritin may involve mitochondrial catabolism, while the export of ferritin from the cells to oligodendrocytes is thought to act through the mediation of ferritin receptors.[27] A possible explanation for the accumulation is that iron transport to the brain appears to be mostly a one-way traffic, i.e. transport into rather than out of the brain.[28,29] Additionally, microstructural changes related to normal ageing (such as e.g. demyelination and tissue rarefication) may release iron that needs to be stored. A recent analysis in healthy subjects demonstrated that iron content in deep GM is also associated with cortical GM volume.[22] This observation could go along with the hypothesis that deep GM is

the storage place of metabolically relevant iron for oligodendrocytes and neurons and therefore scales with the cortical demand. Consequently, this would also suggest a situation where ferritin serving as storage protein keeps iron readily available in a non-toxic way. However, it cannot be excluded that more harmful iron compounds are present as well.

In MS, the association between cortical GM volume and iron accumulation in deep GM seems to revert, i. e. iron could start to accumulate because of decreasing consumption or due to liberation from dying neurons. Furthermore these processes may be modified by disease-related changes of the local milieu as suggested by region-specific associations between the cortical volume and R2* in our study. Previous studies have observed a strong association between cortical GM volume and iron accumulation in deep GM and have interpreted this as a consequence of atrophy due to neurodegeneration.[6,7] Present investigation was not able to replicate such strong relationship between cortical GM volume and iron in deep GM. Significant associations were found for the red nucleus and substantia nigra only. However, previous studies included many more CIS patients and patients at an early stage of the disease.[6,7] This may point to the likelihood of different dynamics of iron accumulation in different stages of the disease.

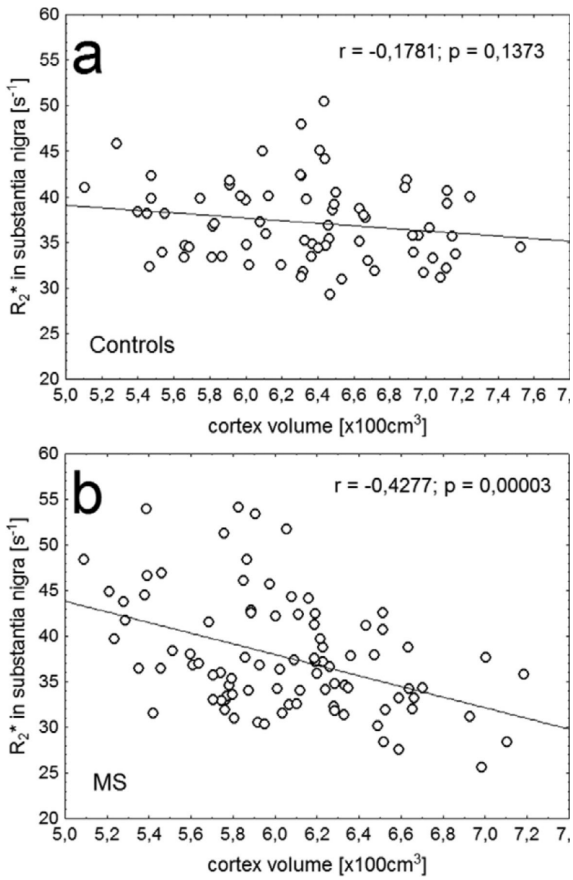

Figure 3. Relationship between cortical grey matter (GM) volume and R2* in the substantia nigra in (a) controls and (b) multiple sclerosis (MS) patients. The negative correlation in the MS patients suggests that disease induced atrophy is linked to an increase of iron in the substantia nigra.

This multicenter study also attempted to provide R2* data on MS lesions. MRI-based iron mapping in WM and in MS lesions still remains a challenge, because the bulk susceptibility of WM is determined by the diamagnetic constituents of the myelin.[30] In addition, the magnetic susceptibility depends on the orientation of the myelinated fibers with respect to the main magnetic field.[31] Therefore, our findings of a reduction of R2* in lesions can be interpreted as evidence for a loss of iron and/or loss of myelin because both produce microscopic field gradients. In fact it appears more likely that the observed association between R2* decrease and disease duration is driven by demyelination which is expected to progress in chronic lesions rather than by a depletion of iron. Because of the much stronger R2* effect of demyelination it could be expected that this might mask even increases in iron levels which have been mostly reported for active lesions in the late stage.[14] In this study, we did not stratify for lesions type but most of the lesions were chronic. Otherwise and in line with our findings there is recent evidence from histopathology that iron content in over 60% of MS lesions is lower than in the surrounding normal appearing white matter.[14]

This study was based on R2* data which were acquired in different centers with different scanners. We recently demonstrated, that the coefficient of variation for the inter-center variability of R2*mapping is less than 6% provided that a standardized protocol is used and an age correction scheme is applied.[22] However, this certainly cannot serve to fully exclude any bias from center effects and the number of patients contributed by individual centers was too small to repeat the analysis by center. In this context it is unlikely that stronger inter-center differences would have caused false positive associations but more subtle associations may have gone undetected. Given the limited number of PP and SP MS patients it has also to be noted that the results of this study were driven primarily by RRMS patients. It is therefore reassuring that the high iron levels observed in deep GM of PP and SPMS patients are in line with all findings. Future studies will need to focus on the dynamics of iron accumulation and specifically on progressive MS. The reliability of future R2* mapping studies could also be increased by the incorporation of than two gradient echoes, an option that was not available for this study in all centers.

Funding
The MS Center Amsterdam is funded by the Dutch MS Research Foundation program grant 09-535c. Iris Kilsdonk is supported by a grant provided by the Noaber Foundation (Lunteren, the Netherlands).

References

1. Bakshi R, Shaikh ZA, Janardhan V. MRI T2 shortening ('black T2') in multiple sclerosis: frequency, location, and clinical correlation. Neuroreport. 2000;11(1):15–21.
2. Bakshi R, Benedict RHB, Bermel RA, et al. T2 hypointensity in the deep gray matter of patients with multiple sclerosis: a quantitative magnetic resonance imaging study. Arch. Neurol. 2002;59(1):62–8.
3. Zhang Y, Zabad RK, Wei X, Metz LM, Hill MD, Mitchell JR. Deep grey matter "black T2" on 3 tesla magnetic resonance imaging correlates with disability in multiple sclerosis. Mult. Scler. 2007;13(7):880–3.
4. Ceccarelli A, Filippi M, Neema M, et al. T2 hypointensity in the deep gray matter of patients with benign multiple sclerosis. Mult. Scler. 2009;15(6):678–86.
5. Hammond KE, Lupo JM, Xu D, et al. Development of a robust method for generating 7.0 T multichannel phase images of the brain with application to normal volunteers and patients with neurological diseases. Neuroimage. 2008;39(4):1682–92.
6. Khalil M, Langkammer C, Ropele S, et al. Determinants of brain iron in multiple sclerosis: a quantitative 3T MRI study. Neurology. 2011;77(18):1691–7.
7. Khalil M, Enzinger C, Langkammer C, et al. Quantitative assessment of brain iron by R(2)* relaxometry in patients with clinically isolated syndrome and relapsing-remitting multiple sclerosis. Mult. Scler. 2009;15(9):1048–54.
8. Zivadinov R, Heininen-Brown M, Schirda CV, et al. Abnormal subcortical deep-gray matter susceptibility-weighted imaging filtered phase measurements in patients with multiple sclerosis: a case-control study. Neuroimage. 2012;59(1):331-9.
9. Craelius W, Migdal MW, Luessenhop CP, Sugar A, Mihalakis I. Iron deposits surrounding multiple sclerosis plaques. Arch. Pathol. Lab. Med. 1982;106(8):397–9.
10. LeVine SM. Iron deposits in multiple sclerosis and Alzheimer's disease brains. Brain Res. 1997;760(1-2):298–303.
11. Haacke EM, Makki M, Ge Y, et al. Characterizing iron deposition in multiple sclerosis lesions using susceptibility weighted imaging. J Magn Reson Imaging. 2009;29(3):537-44.
12. Bagnato F, Hametner S, Yao B, et al. Tracking iron in multiple sclerosis: a combined imaging and histopathological study at 7 Tesla. Brain. 2011;134(Pt 12):3602–15.
13. Wiggermann V, Hernández Torres E, Vavasour IM, et al. Magnetic resonance frequency shifts during acute MS lesion formation. Neurology. 2013;81(3):211–8.
14. Hametner S, Wimmer I, Haider L, Pfeifenbring S, Brück W, Lassmann H. Iron and neurodegeneration in the multiple sclerosis brain. Ann. Neurol. 2013.
15. Hagemeier J, Weinstock-Guttman B, et al. Iron deposition on SWI-filtered phase in the subcortical deep gray matter of patients with clinically isolated syndrome may precede structure-specific atrophy. AJNR Am J Neuroradiol. 2012;33(8):1596-601.
16. Ropele S, de Graaf W, Khalil M, et al. MRI assessment of iron deposition in multiple sclerosis. J. Magn. Reson. Imaging. 2011;34(1):13–21.
17. Langkammer C, Krebs N, Goessler W, et al. Quantitative MR Imaging of Brain Iron : A Postmortem Validation Study. Radiology. 2010;257(2):455–462.
18. Walsh AJ, Lebel RM, Eissa A, et al. Multiple sclerosis: validation of MR imaging for quantification and detection of iron. Radiology. 2013 May;267(2):531-42.
19. Hallgren B, Sourander P. The effect of age on the non-haemin iron in the human brain. J. Neurochem. 1958;3(1):41–51.
20. Jueptner M, Frith CD, Brooks DJ, Frackowiak RS, Passingham RE. Anatomy of motor learning. II. Subcortical structures and learning by trial and error. J Neurophysiol. 1997;77(3):1325-37.
21. Lehéricy S, Bardinet E, Tremblay L, et al. Motor control in basal ganglia circuits using fMRI and brain atlas approaches. Cereb Cortex. 2006;16(2):149-61.
22. Ropele S, Wattjes MP, Langkammer C, et al. Multicenter R2* mapping in the healthy brain. Magn. Reson. Med. 2013.

23. Schweser F, Sommer K, Deistung A, Reichenbach JR. Quantitative susceptibility mapping for investigating subtle susceptibility variations in the human brain. Neuroimage. 2012;62(3):2083–100.
24. Liu J, Liu T, de Rochefort L, et al. Morphology enabled dipole inversion for quantitative susceptibility mapping using structural consistency between the magnitude image and the susceptibility map. Neuroimage. 2012;59(3):2560–8.
25. Connor JR, Benkovic SA. Iron regulation in the brain: histochemical, biochemical, and molecular considerations. Ann. Neurol. 1992;32 Suppl:S51–61.
26. Crichton RR, Wilmet S, Legssyer R, Ward RJ. Molecular and cellular mechanisms of iron homeostasis and toxicity in mammalian cells. J. Inorg. Biochem. 2002;91(1):9–18.
27. Todorich B, Zhang X, Slagle-Webb B, Seaman WE, Connor JR. Tim-2 is the receptor for H-ferritin on oligodendrocytes. J. Neurochem. 2008;107(6):1495–505.
28. Morris CM, Keith AB, Edwardson JA, Pullen RG. Uptake and distribution of iron and transferrin in the adult rat brain. J. Neurochem. 1992;59(1):300–6.
29. Taylor EM, Crowe A, Morgan EH. Transferrin and iron uptake by the brain: effects of altered iron status. J. Neurochem. 1991;57(5):1584–92.
30. He X, Yablonskiy DA. Biophysical mechanisms of phase contrast in gradient echo MRI. Proc. Natl. Acad. Sci. U. S. A. 2009;106(32):13558–13563.
31. Li W, Wu B, Avram A V, Liu C. Magnetic susceptibility anisotropy of human brain in vivo and its molecular underpinnings. Neuroimage. 2012;59(3):2088–97.